# Metamorphic Optoelectronic Integrated Circuits

R.E. Leoni III, C.S. Whelan, P.F. Marsh, Y. Zhang, J.G. Hunt, C.S. Laighton, W.E. Hoke, T.E. Kazior

Raytheon RF Components, 362 Lowell Street, Andover, MA, 01810

*ABSTRACT* — **As the required operational bandwidth of photoreceivers is increased, it becomes desirable to monolithically integrate photodiodes and transistors in order to optimize performance and enhance yield. In this paper we will describe our demonstration of material and process capabilities which allow us to integrate high electron mobility transistors and 1.55 μm P-I-N photodiodes on one substrate. The demonstration vehicles used for this are a dc-45 GHz traveling wave amplifier and a photodiode with 12 μm optical windows. Measured results of three interconnection approaches (standard attenuator, optimized lossy match, buffer amplifier) will be described.**

## I. Introduction

Future generations of defense systems will increasingly take advantage of high speed / wide bandwidth opto-electronic components operating at 1.55 μm wavelengths for both digital and analog links [1]-[3]. Digital links in excess of 50 Gbps are expected to make up the back planes of future phased arrays. Also, high spur-free dynamic range analog optical links will provide interference free, easy to make and break connections which will drive down costs and increase flexibility in future mobile systems.

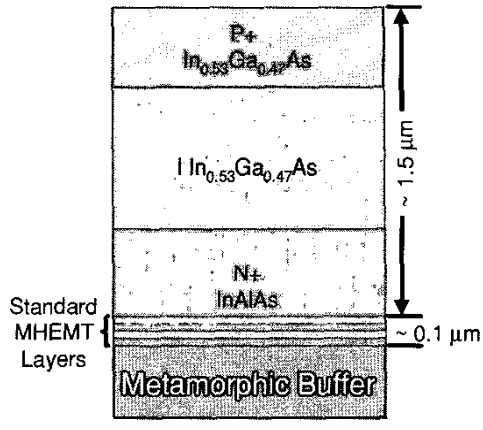


Fig. 1. Metamorphic OEIC material stack consisting of vertical PIN and standard low noise HEMT layers.

HEMTs are more attractive than HBTs for these high sensitivity and wide bandwidth applications. They have much better RF noise performance than HBTs [4]. Also, reduction of device parasitics through scaling of HEMT dimensions is relatively easy to implement. Noise figures of 3 dB at 95 GHz and $F_{MAX}$'s of 400 GHz are not unusual for short gate length InP and metamorphic HEMTs [5].

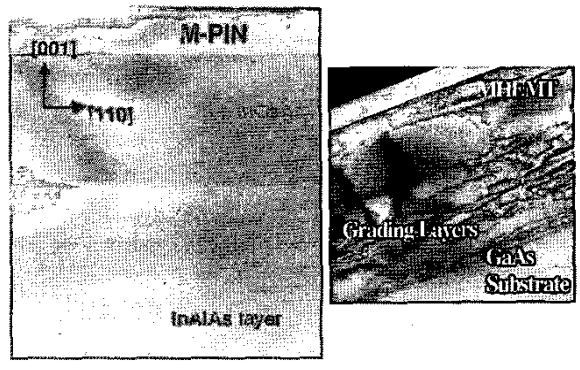


Fig. 2. TEM micrographs of metamorphic PIN material layers (left), and HEMT active layers on top of the metamorphic buffer (right). While the buffer layers contains a large amount of defects, very few propagate into the active layer.

In order to truly take advantage of the low noise and high frequency performance of HEMTs in photoreceiver circuitry it is necessary to monolithically integrate them with photodiodes. Optoelectronic integrated circuits (OEICs) allow performance to be optimized for the particular requirements of a link. Also, a much more reproducible photoreceiver is created by controlling the interface between the photodiode and pre-amplifier on chip rather than using a hybrid approach. The following paper describes Raytheon RF Components' OEIC process that integrates vertical PIN photodiodes [6] and HEMTs [7] which has been developed to address future defense system needs for high performance optical receivers.

## II. Material and Device Fabrication

The active layers of the OEIC material structure were grown on metamorphic GaAs substrates using MBE. Metamorphic buffer technology allows the deposition of layers with virtually any indium content on GaAs without the defects associated with lattice mismatch. By grading the indium content over the 1.5 μm thickness of the AlInGaAs buffer layer, the lattice constant is transformed.



0-7803-7695-1/03/$17.00 © 2003 IEEE

[8], Raytheon RF Components and other companies have successfully used this technology to manufacture low cost, high performance InP-like HEMTs in production quantities [9].

Typically OEIC material stacks are simply HBT's [10]-[12] in which the base-collector junction also serves as the photodiode. This compromises both photodiode and transistor performance. The OEIC material for the implementation described in this paper consists of an optimized PIN photodiode stack on top of standard low noise HEMT layers. As illustrated in Fig. 1, the PIN diode is composed of InGaAs P+ and intrinsic layers on top of an N+ InAlAs layer. The critical layers of the HEMT underneath are an N+ $In_{0.53}Ga_{0.47}As$ cap, N InAlAs Schottky, and a 200Å $In_{0.53}Ga_{0.47}As$ channel.

The metamorphic buffer used for OEIC structures provides lattice transformation with little if any residual strain in the thick $In_{0.53}Ga_{0.47}As$ layers of a PIN diode. Fig. 2 shows a TEM micrograph of photodiode active layers. Few if any dislocations are observed. A plot of dark current as a function of diode diameter further illustrates the material quality (Fig. 3). Both InP and metamorphic diodes have approximately the same leakage currents, and they exhibit a roughly linear relationship between dark current and diameter. This is an indication that the current is dominated by surface leakage (periphery dependent) rather than bulk defects (area dependent).

The OEIC process required the melding of both PIN and HEMT processes. Due to the overlap of a number of steps only three additional mask layers beyond the standard MHEMT mask set were necessary (anode mesa, cathode mesa, and AR coat). Selective etching was used to define all critical mesa structures and to create the single-wide recess of the low-noise HEMTs. The standard transistor ohmic, metal, nitride capacitor, and via processes were used. Thanks to the relatively thin HEMT layers, the air bridge height from substrate to anode was only slightly longer and did not impact yield.

Neither transistor nor photodiode performance were negatively impacted by merging the two processes. Unpackaged photodiodes with 12 μm optical windows had typical responsivities of 0.5 A/W and ~3 dB bandwidths of approximately 28 GHz. This compares well with state-of-the-art performance of stand alone, unpackaged InP photodiodes of similar size (Fig. 4). When packaged and fibered efficiently, the stand alone InP and metamorphic GaAs photodiodes have 3 dB bandwidths in excess of 50 GHz in a 50 Ω system and typical responsivities of 0.7 A/W. A comparison of HEMT characteristics extracted after gate deposition is shown in Table I. The lines in the graphs mark upper and lower process limits for the standard 0.15 μm gate length metamorphic HEMT.

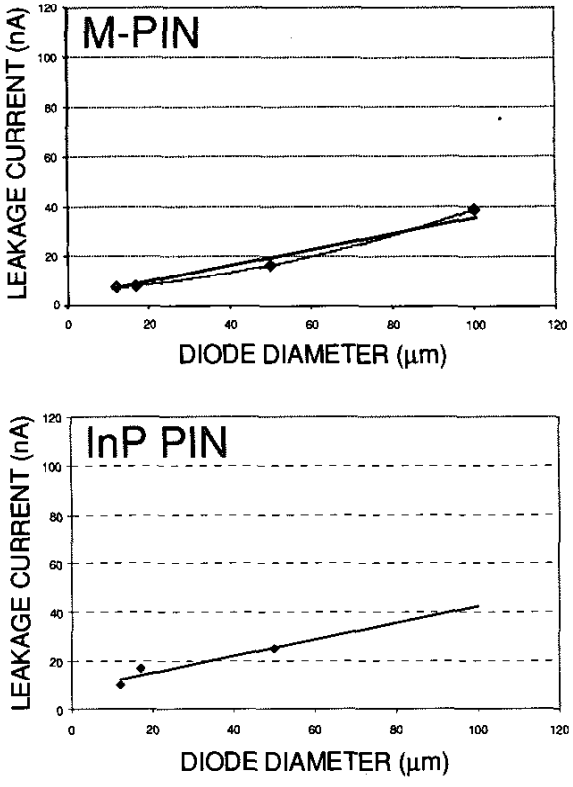


Fig. 3. Leakage current dependence on diode diameter for metamorphic GaAs (top) and InP (bottom) vertical PIN photodiodes. Note that the InP and metamorphic devices have approximately the same leakage current. Both data sets have a roughly linear relationship between leakage and diode diameter indicating surface rather than bulk leakage paths dominate.

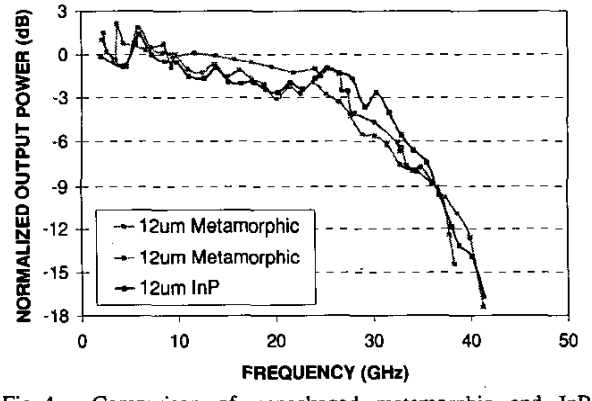


Fig. 4. Comparison of unpackaged metamorphic and InP photodiode frequency performance. Both device types have approximately the same responsivity and frequency response.

TABLE I
Comparison of median OEIC transistor characteristics with standard HEMT

| | Idss (mA/mm) | Peak Gm (mS/mm) | Rs (Ω·mm) | Vpo (V) |
|---|---|---|---|---|
| Standard | 525 | 850 | 0.35 | -0.78 |
| OEIC Wfr1 | 530 | 860 | 0.38 | -0.80 |
| OEIC Wfr2 | 610 | 900 | 0.33 | -0.85 |

## III. OEIC DESIGN AND RESULTS

A dc-45 GHz traveling wave amplifier was chosen as a base preamplifier for the metamorphic OEIC development. The circuit is described in detail elsewhere [13]. In brief, in a 50 Ω system the circuit provides 16 ± 0.75 dB of gain over the entire band. Input and output return losses were better than 8 dB.

The electrical parasitics for the photodiode model were extracted from the 1-port s-parameters of a stand-alone metamorphic PIN. Although photocurrent production is a nonlinear process, it is adequate to use a voltage dependent current source to model it. This assumes a constant, frequency independent optical input power. A 50 Ω termination in the input of source ensures full absorption of incident power. Responsivity was treated as a scaling factor and the dependent current source's transconductance was set to 1 A/V in the model. Fig. 5 shows the final photodiode model including parameter values.

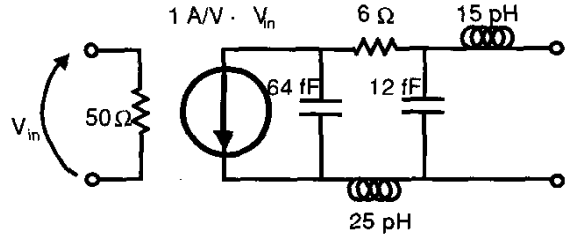


Fig. 5. 2-port photodiode lumped element model and parameter values for a 10 μm optical window diode. The transconductance of the dependent current source may be changed to account for the expected responsivity.

No modifications were made to the traveling wave amplifier for the purposes of optimizing photoreceiver performance. Instead, wide bandwidth interconnection techniques were investigated. Three approaches were taken including a standard 50 Ω matched 5 dB attenuator, a lossy matching network, and a common source buffer amplifier. The later two topologies were optimized in LIBRA [14] using measured s-parameters for the traveling wave amplifier and the 2-port photodiode model. The alternative lossy match consists of a resistive / inductive path to ground that helps react out the diode capacitance as well as match to the traveling wave amplifier.

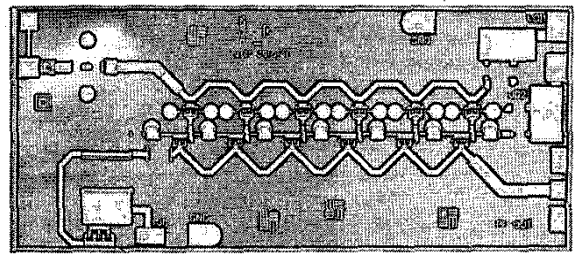

Fig. 6. Photograph of a metamorphic OEIC consisting of a photodiode, 5 dB attenuator, and a traveling wave amplifier.

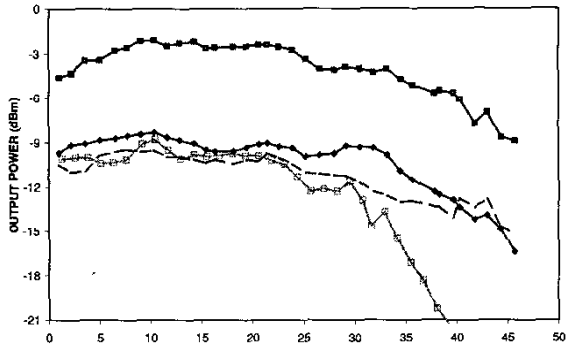


Fig. 7. Measured frequency response of four photoreceiver configurations. The photodiode – amplifier interconnections are made using (–□–) hybrid lossy match, (—) monolithic 5 dB attenuator, (–◆–) monolithic lossy match, (–■–) monolithic buffer amplifier. All measurements were performed with the same optical input power.

Fig. 6 is a photograph of a fabricated OEIC with the 5 dB attenuator interconnect. A comparison of the various configurations' measured results for a given optical input power is displayed in Fig. 7. Included in the figure is a result for a hybrid photoreceiver composed of a stand-alone photodiode and the traveling wave amplifier. The hybrid uses a lossy match to interface with the amplifier. Measurements were performed without packaging the devices. The course manual alignment of the optical fiber results in less than optimal responsivity, but is adequate to determine the relative merits of the interconnect approaches. All of the monolithic solutions provide approximately 38 GHz of bandwidth, which is approximately 20% greater than the hybrid approach. This is due to the lower, better-controlled parasitics of the monolithic implementation. The common source buffer amplifier configuration provides over 5 dB higher gain as expected. In addition to better performance, the OEIC is

extremely reproducible. Fig. 8 presents an overlay of the normalized transfer characteristics of 5 OEICs. In general the shape of the transfer characteristics are identical, with a worst-case difference of 1.5 dB.

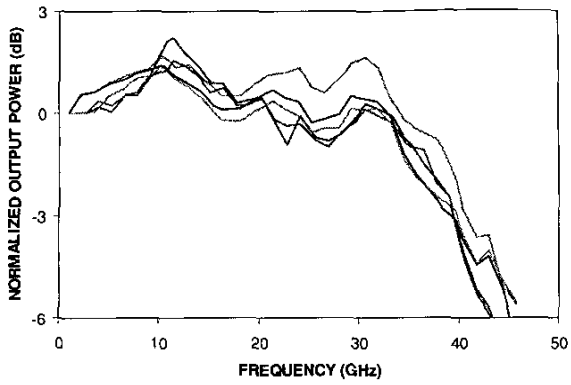


Fig. 8. Overlaid frequency response of 5 lossy matched OEICs from the same wafer. Note that for most frequencies and devices, the differences could be attributed to variations in measurement.

## IV. Conclusion

A metamorphic GaAs based OEIC process has been developed at Raytheon RF Components to address future high performance photoreceiver needs around 1.55 μm operating wavelengths. Rather than monolithically integrating HBTs and photodiode structures, OEICs consisting of high electron mobility transistors and vertical P-I-N photodiodes were fabricated in order to take advantage of the excellent noise and high frequency capabilities of metamorphic HEMTs. OEIC demonstration vehicles consisting of a traveling wave amplifier, a photodiode with 12 μm optical windows and various interconnect approaches resulted in high performance, wide-bandwidth (~38 GHz) photoreceivers. These devices demonstrate the excellent reproducibility and reduced parasitics that may be attained through monolithic integration.

## References


[1] E. I. Ackerman, C. H. Cox, "RF fiber-optic link performance," *IEEE Microwave Magazine*, Vol. 2, Iss. 4, pp. 50-58, Dec. 2001.

[2] Y. Chen, R T. Chen, "A fully packaged true time delay module for a K-band phased array antenna system demonstration," *IEEE Photonics Technology Letters*, Vol. 14, Iss. 8, pp. 1175-1177, Aug. 2002.

[3] J. Onnegren, L. Pettersson, "Optical distribution of reference signals to a digital beamforming antenna," *1998 Inter. Topical Meeting on Microwave Photonics*, pp. 119-122, Oct. 1998.

[4] L. Tran, J. Cowles, R. Lai, T. Block, P. Liu, A. Oki, D. Streit, "Monolithic integration of InP HBT and HEMT by selective molecular beam epitaxy," *1996 Inter. Conf. on Indium Phosphide and Related Materials*, pp. 76-78, April 1996.

[5] P. M. Smith, K. Nichols, W. Kong, L. MtPleasant, D. Pritchard, R. Lender, J. Fisher, R. Actis, D. Dugas, D. Meharry, and A. W. Swanson, "Advances in InP HEMT Technology for High Frequency Applications," *GaAs IC Symp. Dig.*, pp. 7-10, Oct. 2001.

[6] C. S. Whelan, P F. Marsh, R. E. Leoni III, J. Hunt, M. Griegas, W. E. Hoke, KC Hwang, and T. E. Kazior, "Metamorphic PIN Photodiodes for the 40 Gb/s Fiber Market," *2001 GaAs IC Symp. Dig.*, pp. 251-254, Oct. 2001.

[7] R. E. Leoni III, W. E. Hoke, C. S. Whelan, P. F. Marsh, P. C. Balas II, J. G. Hunt, K. C. Hwang, S. M. Lardizabal, C. Laighton, S. J. Lichwala, Y. Zhang, and T. E. Kazior, "GaAs-based metamorphic technology," *Inter. Conf. on GaAs Man. Tech.*, pp. 272-275, May 2002.

[8] W. E. Hoke, P. J. Lemonias, J. J. Mosca, P. S. Lyman, A. Torabi, P. F. Marsh, R. A. McTaggart, S. M. Lardizabal, K. Hetzler, "MBE growth and device performance of metamorphic high electron mobility structures fabricated on GaAs substrates," *J. Vacuum Science & Tech. B*, 17 (3) 1999, pp. 1131-1135.

[9] C. S. Whelan, P. C. Balas, P. F. Marsh, R. E. Leoni, W. E. Hoke, T. E. Kazior, L. A. Aucoin, "Production of MHEMTs for microwave and millimeter-wave applications," *2001 CS-MAX Conf. Proc.*, pp. 40-44, July 2001.

[10] T. P. E. Broekaert, J. F. Jensen, D. Yap, D. L. Persechini, S. Bourgholtzer, C. H. Fields, Y. K. Brown-Boegeman, B. Shi, R. H. Walden, "InP-HBT optoelectronic integrated circuits for photonic analog-to-digital conversion," *IEEE Jour. of Solid-State Circuits*, Vol. 36, Iss. 9, pp. 1335-1342, Sept. 2001.

[11] D. Huber, R. Bauknecht, C. Bergamaschi, M. Bitter, A. Huber, T. Morf, A. Neiger, M. Rohner, I. Schnyder, V. Schwarz, A. Jackel, "InP-InGaAs single HBT technology for photoreceiver OEIC's at 40 Gb/s and beyond," *Jour. of Lightwave Technology*, Vol. 18, Iss. 7, pp. 992-1000, July 2000.

[12] B. Willen, U. Eriksson, P. Evaldsson, D. Haga, M. Mokhtari, U. Westergren, "InP HBT technology for high speed circuits and OEICs," *Proc. of the 1997 Inter. Conf on Indium Phosphide and Related Materials*, pp. 620-632, May 1997.

[13] R. E. Leoni III, S. J. Lichwala, J. G. Hunt, C. S. Whelan, P. F. Marsh, W. E. Hoke, and T. E. Kazior, "A DC – 45 GHz metamorphic HEMT traveling wave amplifier," *2001 GaAs IC Symp. Dig.*, pp. 133-136, Oct. 2001.

[14] Agilent Technologies Inc., Westlake, CA.